

A novel quasi-distributed fibre optic displacement sensor for dynamic measurement

This article has been downloaded from IOPscience. Please scroll down to see the full text article.

2010 Meas. Sci. Technol. 21 075205

(<http://iopscience.iop.org/0957-0233/21/7/075205>)

View [the table of contents for this issue](#), or go to the [journal homepage](#) for more

Download details:

IP Address: 222.197.180.159

The article was downloaded on 11/03/2011 at 02:10

Please note that [terms and conditions apply](#).

A novel quasi-distributed fibre optic displacement sensor for dynamic measurement

Sascha Liehr and Katerina Krebber

BAM Federal Institute for Materials Research and Testing, Unter den Eichen 87, 12205 Berlin, Germany

E-mail: Sascha.Liehr@bam.de

Received 18 December 2009, in final form 16 April 2010

Published 15 June 2010

Online at stacks.iop.org/MST/21/075205

Abstract

We present a novel technique based on incoherent optical frequency domain reflectometry (OFDR) to measure length changes quasi-distributed between reflection points in optical fibres. The technique enables length changes to be measured with a resolution better than 1 μm and allows for static and dynamic measurement capabilities up to 2 kHz. We demonstrate that dynamic measurements of multiple fibre sections can be conducted independently from each other with high precision. Due to the precise and dynamic measurement capabilities, the proposed sensor system is expected to open new fields of application, especially in the structural-health-monitoring sector. Possible applications are discussed in the paper.

Keywords: strain sensor, optical frequency domain reflectometry, OFDR, optical fibre, fibre sensors, quasi-distributed sensors, dynamic strain measurement

(Some figures in this article are in colour only in the electronic version)

1. Introduction

During the last two decades, the development of fibre optic sensors has made substantial progress and numerous sensor systems have successfully been commercialized. Especially in the structural-health-monitoring (SHM) sector, fibre optic sensors found application in structural surveillance and damage detection. Distributed fibre optic strain sensors based on Brillouin scattering [1] allow for precise measurement of strain up to several tens of km. Sensor systems based on swept-wavelength interferometry [2] enable precise distributed strain measurement for moderate lengths. Another coherent strain sensing technique for limited fibre lengths has been proposed [3]. The use of polymer optical fibre (POF) OTDR [4] or OFDR [5, 6] techniques for distributed measurement of very high strain up to 40% and absolute length change measurement have been proposed. All distributed systems, however, are not suitable to monitor dynamic processes > 1 Hz because of too long acquisition times.

There is an increasing necessity and growing market for monitoring the dynamic behaviour of structures. Especially in transportation (aviation, aeronautics, naval), civil

infrastructure (bridges) or structural components (wind turbine blades), instant damage detection, modal behaviour, creep or load cycle information is important.

Notably fibre Bragg grating (FBG) sensors are suitable to measure local strain at high frequencies. However, the gauge length of this quasi-distributed sensor system is basically limited to the grating length. Packaging solutions to extend the gauge length to several metres have been proposed. Another technique based on in-fibre long-gauge Michelson interferometers (SOFO) provides precise static and dynamic strain measurement up to a 20 m gauge length [7]. Both FBG and SOFO systems provide excellent solutions to precisely measure local strain but require rather expensive sensors and interrogation units and have limited applicability for certain applications, especially when long-gauge measurement is necessary. Recently presented strain sensors using phase measurement techniques [8] enable precise and dynamic strain measurement of the whole length of an optical fibre. This sensor type is favourable for long-gauge applications but only one fibre section per channel can be interrogated.

The following introduced sensor system presents an alternative to these sensor systems and promises new

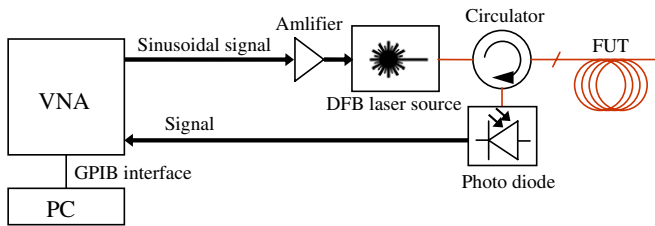


Figure 1. Schematic of the OFDR setup.

applications in structural health monitoring. We propose, for the first time to our knowledge, a sensor system that allows for very precise static and dynamic length change or strain measurement between multiple reflection points along a single fibre. The sensor application is straightforward, flexible and low cost since the fibre itself is the sensor and can easily be conditioned on site. For example standard 0° -physical contact connectors can act as reflection points dividing the fibre into single sensor sections. The gauge length can be chosen from centimetres to kilometres by simple bonding or integration of the fibre sections into any structure.

In the following, the measurement principle and signal processing algorithms will be explained. The current precision and dynamic performance of the sensor system are shown and we demonstrate that standard FC/PC connectors as reflection points can be used to monitor dynamic oscillation of a cantilever beam.

2. Sensor principle

2.1. OFDR technique

The sensor principle is based on the optical frequency domain reflectometry (OFDR) technique. We already demonstrated the possibility of measuring the backscatter signal of silica fibres and detecting distributed strain in polymer optical fibres (POF) using OFDR [5, 6]. The backscatter signal of the fibre under test (FUT) can be obtained by measuring the complex transfer function (TF) in the frequency domain over a wide frequency span and calculating the pulse response in the time domain by conducting an inverse fast Fourier transform (IFFT). The laboratory setup is shown in figure 1. A vector network analyser (VNA) generates a sinusoidal signal and enables sweeping over a wide frequency band measuring the complex transfer function of the setup.

The sinusoidal signal from the VNA is amplified by a wide-band electrical amplifier and fed to a bias-T circuit of a 1310 nm distributed feedback (DFB) continuous-wave laser source with a maximum power of 31 mW. The amplitude-modulated laser signal is then coupled to the FUT using an optical circulator. All backscattered and back-reflected light of the FUT is received by a photodiode and the resulting electrical signal is fed to the VNA to measure the complex transfer function of the setup. Frequency sweeping, data transfer from the VNA, calculation of the calibrated signal, signal processing, IFFT and display of the backscatter signal in the time domain are fully controlled and obtained by an external PC. The current sweep frequency range of the

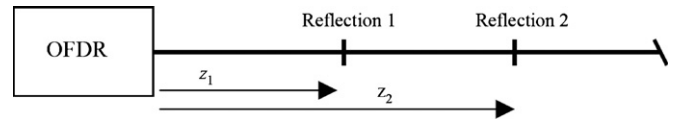


Figure 2. Schematic of the FUT with two reflections.

setup for amplitude modulation is 9 kHz to 2 GHz. The overall cost of the sensor system can be considerably reduced by replacing the VNA and using digital data acquisition techniques [9].

2.2. Length change measurement technique

Having conducted an OFDR measurement, the impulse response of the fibre in the time domain as well as the frequency domain data for each swept frequency point is known. Each measured frequency point contains information on the whole FUT. The idea is to extract important reflection characteristics of the FUT in the frequency domain by time domain filtering and to reconstruct updated reflection characteristics from a new measurement of only a few points in the frequency domain. In the following, a simple example of this technique to measure the length change of two fibre sections between reflection points in the fibre is explained. Figure 2 shows the schematic of the setup.

The OFDR setup is connected to the FUT with two strong reflections originating from physical contact connectors at the distances z_1 and z_2 . The reflection of the fibre end is suppressed with an angle-polished connector. The first step is to measure the frequency domain response of the FUT. The transfer function $H(f)$ of the FUT is shown in figure 3(a). Both connector reflections can clearly be seen in the time domain depiction $h(z)$ in figure 3(b) after conducting an IFFT with $H(f)$.

From the time domain data, the position of the reflections z_1 and z_2 can be determined with high precision. In the following, the single reflection components $h_1(z)$ and $h_2(z)$ are 'cut out' of $h(z)$ by setting every h -value apart from the reflections to zero (figure 4).

The time domain data of the fibre without any reflection $h_0(z)$ is then calculated by subtracting the single reflections from $h(z)$. The general description for n reflections with $h_r(z)$, $r \in \{1, \dots, n\}$, is

$$h_0(z) = h(z) - \sum_{r=1}^n h_r(z). \quad (1)$$

The frequency domain response of all reflections $H_r(f)$ and $H_0(f)$ is calculated from the time domain data of the single reflections $h_r(z)$ and $h_0(z)$ using FFT (figure 5).

Now $H_r(f)$, the absolute values $|H_r(f)|$ and phase values $\varphi_r(f)$, $r \in \{1, \dots, n\}$, of all n reflections and each measurement frequency f as well as $H_0(f)$ are known and will be used for further calculations as a reference measurement.

The results of new measured frequency points $M(f_k)$ of the FUT at arbitrary frequencies f_k with $k \in \{1, \dots, n\}$ correspond to the sum of all reflections $H_r(f_k)$ and $H_0(f_k)$ at the measured frequencies f_k in the frequency domain. For each frequency

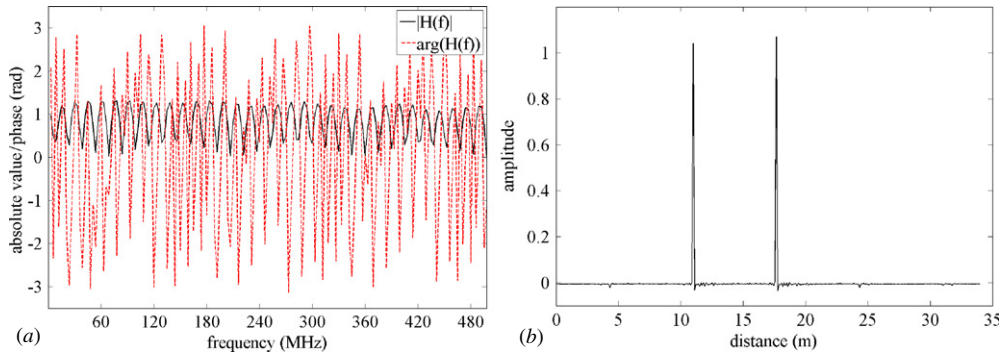


Figure 3. (a) Transfer function of the FUT $H(f)$ (absolute value and phase) and (b) impulse response $h(z)$ of the FUT with two reflections at the positions z_1 and z_2 .

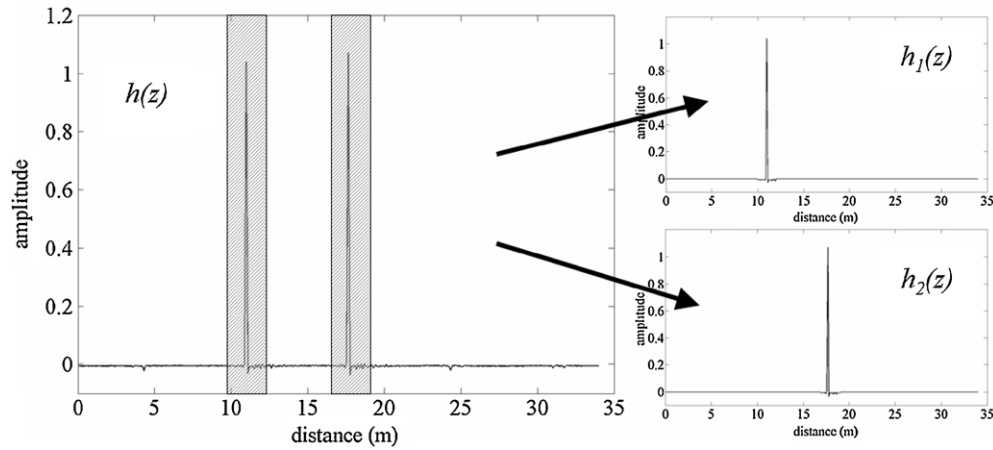


Figure 4. ‘Cutting out’ the single reflections from $h(z)$ resulting in $h_1(z)$ and $h_2(z)$.

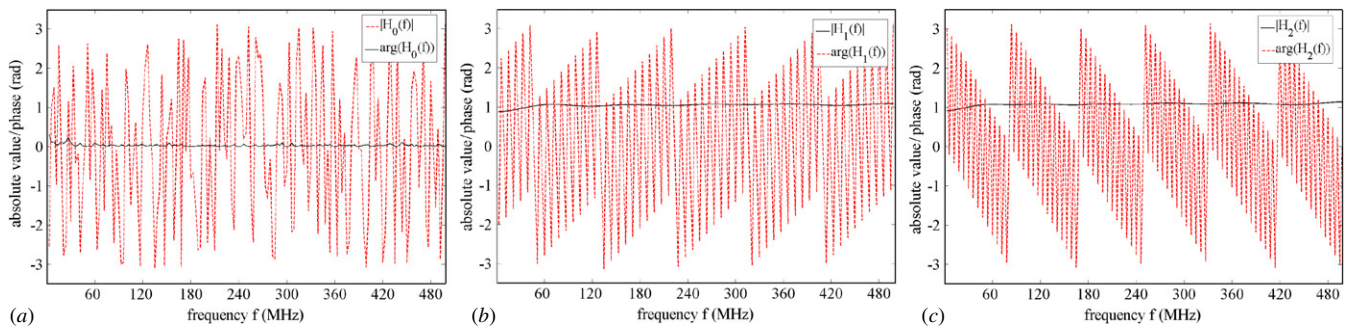


Figure 5. Frequency domain data: (a) $H_0(f)$, (b) $H_1(f)$ and (c) $H_2(f)$.

f_k , a length change of a fibre section relative to the reference measurement Δz_r would result in a phase change $\Delta\varphi_r$ for each single reflection. $\Delta\varphi_r$ is therefore the parameter to determine the relative length change for each reflection Δz_r . With the information obtained from the filtering in the time domain one can define a complex-valued system of equations in the frequency domain with n lines and n columns to calculate the particular phase φ_{rk} and absolute value $|H_{rk}|$ for each reflection and frequency. Only n measurements $M(f_{k=1\dots n})$ are necessary to determine the phase φ_{rk} of all n reflections. The system of equations for the example of two reflections measured at arbitrary frequencies $f_{k=1}$ and $f_{k=2}$ ($f_{k=2} >$

$f_{k=1}$) is

$$\begin{aligned} \text{I } M(f_{k=1}) - H_0(f_{k=1}) &= |H_1(f_{k=1})|e^{i(\varphi_{11})} + |H_2(f_{k=1})|e^{i(\varphi_{21})} \\ \text{II } M(f_{k=2}) - H_0(f_{k=2}) &= |H_1(f_{k=2})|e^{i(\varphi_{12})} + |H_2(f_{k=2})|e^{i(\varphi_{22})}. \end{aligned} \quad (2)$$

All phase values φ_{rk} for each reflection depend on the measurement frequency f_k and the distance of each reflection z_r . All φ_{rk} can be related to the phase values $\varphi_{rk=1}$ at the frequency $f_{k=1}$ (hereafter named φ_r) using the value Δ_{rk} :

$$\varphi_{rk} = \varphi_r - \Delta_{rk}. \quad (3)$$

Each Δ_{rk} is the calculated relative phase difference between the measurements with the frequency $f_{k=1}$ and

frequency f_k and is a function of the reflection position z_r and the frequency difference $\Delta f = f_k - f_1$:

$$\Delta z_r = 4\pi \cdot \Delta f \cdot z_r \frac{n_{gr}}{c_0}, \quad (4)$$

where c_0 is the speed of light and n_{gr} is the group refractive index of the fibre. As only the reflection components of the fibre are used for the calculation, the previously calculated $H_0(f_k)$ component for each frequency has to be subtracted from the new measurement value $M(f_k)$.

The accuracy of the measurement can be further increased by using an over-determined system of equations with m ($m > n$) measured frequency points $M(f_k) \ k \in \{1, \dots, m\}$. The system of equations for the general case with n reflections in the fibre and m measured frequency points is

$$\begin{aligned} f_{k=1} \text{I} M(f_k) - H_0(f_k) &= |H_{r=1}(f_{k=1})| e^{i(\varphi_{r=1})} \\ \vdots & \vdots \\ f_{k=m} \text{II} M(f_{k=m}) - H_0(f_{k=m}) &= |H_{r=1}(f_{k=m})| e^{i(\varphi_{r=1} - \Delta_{r=1,k=m})} \end{aligned}$$

In the following, the system of equations is solved and the phase information of each reflection $e^{i\varphi_r}$ at the frequency $f_{k=1}$ is calculated. The phase change of each reflection $\Delta\varphi_r$ at the time of a new measurement relative to the reference measurement for example can be calculated from $e^{i\varphi_r}$ and $H_r(f_{k=1})$. From $\Delta\varphi_r$, the resulting length changes of all fibre sections Δz_r can be obtained using

$$\Delta z_r = \frac{\Delta\varphi_r}{4\pi \cdot f_{k=1}} \cdot \frac{c_0}{n_{gr}}. \quad (6)$$

Since z_r is used as a starting value to calculate Δz_r , the change of z_r introduces a deviation from the correct value. The resulting error of Δz_r , however, can be eliminated by a few iteration steps using a new $z_{r(\text{new})} = z_r + \Delta z_r$ as a starting value.

Due to the possibility of calculating absolute length changes between n reflection points from a few measurement points in the frequency domain only, the measurement repetition rate can be significantly increased. Another advantage of this technique compared to simple phase measurement techniques [8] is that the measurement range is not limited by the interrogation frequency but by the lowest frequency $f_{k=1}$ used for the calculation. Since any frequency point can be used for the measurement, the measurable range can be very wide:

$$\Delta z_{\text{max}} = \frac{1}{4\pi \cdot f_{k=1}} \cdot \frac{c_0}{n_{gr}} \cdot (\pm\pi). \quad (7)$$

Moreover, the solution of the system of equations is not affected by changes of the reflected optical powers at the connectors. That means optical loss induced along the fibre or changes at the connectors provide the same phase result as long as the relation of the $|H_r|$ over the measured frequency remains constant. This also means that the phase φ_r and the absolute value $|H_r| \cdot |e^{i\varphi_r}|$ of each reflection can be obtained simultaneously and independently. This possibility of measuring phase and reflected optical power at once yields a multitude of new sensing applications. In the following section only quasi-distributed strain measurement is presented.

3. Measurement results

All measurement results presented in the following are conducted with standard single-mode optical fibres, but multimode fibres or polymer optical fibres can equally be used. In order to demonstrate the functionality of the system, a simple experiment with a two-section sensor, as shown in figure 2, has been conducted. Each section is about 20 m long and terminated by a strongly reflecting physical contact connector. The length of the first fibre section was maintained whereas a 50 cm part of the second fibre section was strained in steps using a PC-controlled step motor setup. The two ends of the short strained section have been glued onto a metallic surface. The 25 μm steps applied by the step motor resulted

$$\begin{aligned} + \dots + |H_{r=n}(f_{k=1})| e^{i(\varphi_{r=n})} \\ + \dots + \vdots \\ + \dots + |H_{r=n}(f_{k=m})| e^{i(\varphi_{r=n} - \Delta_{r=n,k=m})}. \end{aligned} \quad (5)$$

in an actual length change of 19.2 μm per step owing to the glue's elasticity. Figure 6 shows the absolute measured length change of the elongated fibre section.

The results show that the length change can be measured with μm resolution.

To demonstrate that the length change of multiple fibre sections can be measured dynamically and independently of each other with high precision, a demonstration setup with four 15 m long sensor sections has been built. Figure 7 shows the 5 mm thin wooden panel with two pre-strained fibre sections bonded on each side of the panel. One end of the panel is fixed so that when the plate is deflected, the two fibre sections on one side of the panel are tensioned whereas the fibres on the back-side are compressed. Figure 7 shows an example measurement of the panel in static condition at $t < 1$ s, deflected in one direction from $t = 1$ s to 3.2 s and a free damped oscillation of the panel for $t > 3.2$ s.

This demonstration measurement clearly shows that multiple fibre sections can be monitored independently with high precision. The length change values of all fibre sections agree well in magnitude and sign with the expected behaviour. In an actual monitoring application, a single sensor fibre with multiple sections can be used to dynamically and independently measure the deformation of different parts of a structure in real time. Each length change result can distinctly be allocated to the respective monitoring zone.

The sensor system is expected to be very flexible in application since the length of each fibre section can be chosen according to the requirements, and the number of sensor sections is theoretically unlimited. Another advantage of the proposed technique is that precise length change measurement can be combined with high measurement frequencies. Both qualities, measurement speed and, with inverse dependence, the measurement precision, are a function of various parameters such as the filter bandwidth of the VNA, the degree of overdetermination of the system of equations and averaging. The maximum possible measurement frequency is basically limited by the measurement speed of the VNA

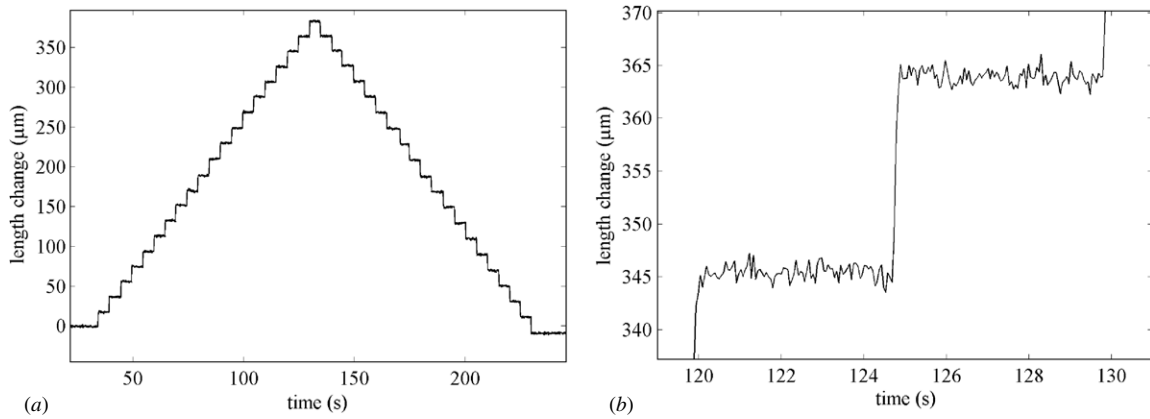


Figure 6. (a) Measurement of second fibre section strained in steps of $19.2 \mu\text{m}$ and (b) detail of the same measurement (measurement rate 20 Hz, $n = 2$, $m = 10$).

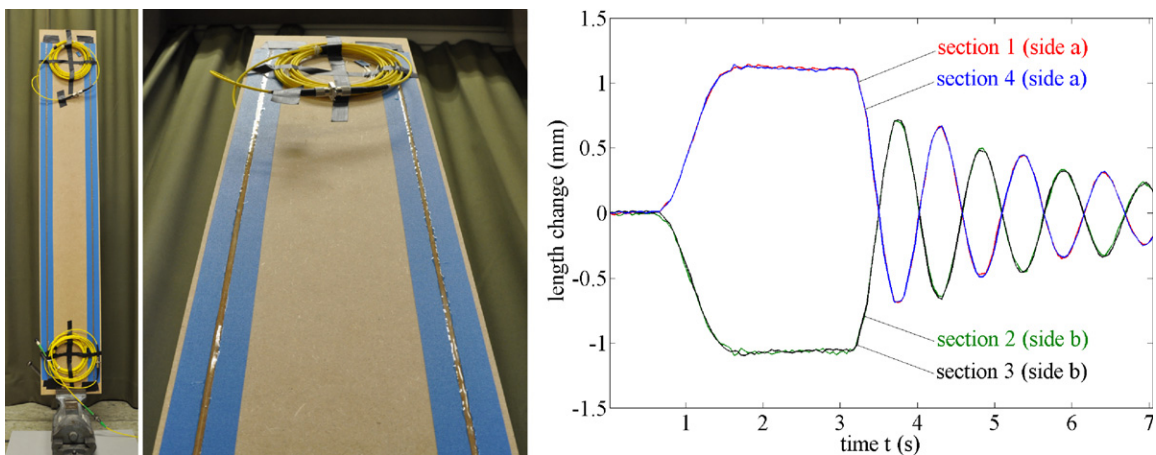


Figure 7. Demonstrator set-up (left) and the result of a dynamic measurement with two strained/compressed fibre sections in static condition $t < 1$ s, deflected in one direction from $t > 1$ s to 3.2 s and a free damped oscillation for $t > 3.2$ s (right).

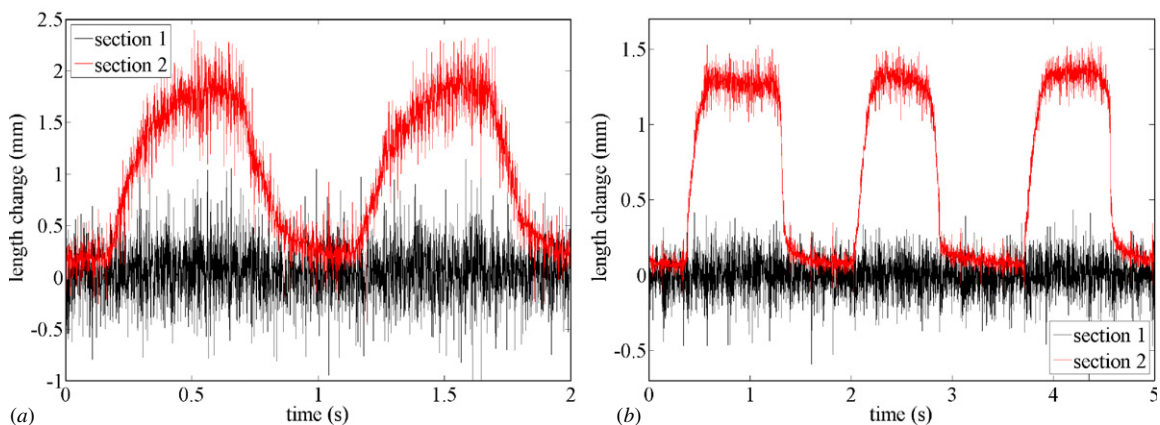


Figure 8. Length change measurement of a two-section sensor with section one unstrained, and strain applied to section 2 at a measurement rate of (a) 2 kHz ($n = 2$, $m = 2$) and (b) 1 kHz ($n = 2$, $m = 4$).

and the communication speed between the VNA and the PC. Figure 8(a) shows a measurement with the currently highest possible measurement repetition rate of 2 kHz and figure 8(b) shows a measurement of the same fibre using an over-determined system of equations with $n = 2$ and $m = 4$.

Optimization of the signal processing and device communication will further extend the measurement dynamics. Alternatively, the measurement accuracy can be increased at the expense of the measurement frequency by decreasing filter bandwidth and increasing averaging and overdetermination of the equation system. An example of

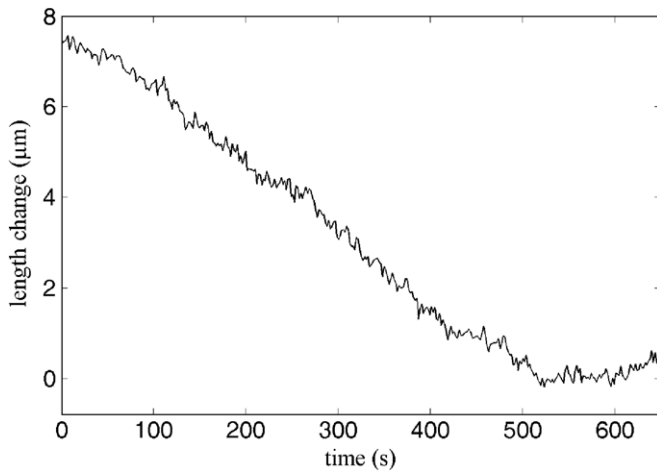


Figure 9. High-accuracy measurement at 0.6 Hz.

a high-resolution measurement with a repetition rate of about 0.6 Hz is shown in figure 9.

The figure shows that the length change resolution is better than $1\ \mu\text{m}$ and even higher resolution is possible when the measurement speed is further decreased. This is, to our knowledge, the highest reported resolution for non-interferometric measurement systems.

The drift of the measurement signal in the figure is not due to strain but temperature and indicates that the temperature-introduced length change and refractive index change of the fibre might be an issue when high-precision measurement is required. These temperature effects, however, can be compensated by installing a strain-free section as a temperature reference next to the strain fibre. In this way temperature and strain can be discriminated and measured separately.

As this technique has been presented to measure the displacement between reflection points in the fibre by calculating the phase information for each reflection, the reflected optical power at each connector or fibre end can also be calculated. This enables simultaneous measurement of length changes and for example refractive indices, absorption coefficients or optical loss quasi-distributed along the fibre or at open fibre ends. First experiments proved that for example refractive index changes at multiple open fibre ends and their displacements can be measured simultaneously. Results on that topic will be presented in the future.

4. Conclusion

We have presented a novel technique based on the incoherent optical frequency domain reflectometry (OFDR) technique to precisely measure length changes quasi-distributed between multiple reflections in optical fibres at frequencies up to 2 kHz. Measurement results with single-mode optical fibres have been presented but the technique equally works in multimode fibres

or polymer optical fibres. The measurement resolution of less than $1\ \mu\text{m}$ is, to our knowledge, the highest reported for non-interferometric systems. Laboratory measurements proved that the proposed technique is applicable in practice and multiple fibre sections can be monitored independently of each other with high resolution and measurement rate. The proposed technique allows for new applications especially in the field of structural health monitoring. Length changes and deformations of structures and components can be measured precisely and dynamically by simply bonding the fibre to the sections of interest. The sensor system is very flexible in application since the gauge length can be chosen from centimetres to kilometres and any number of standard physical contact connectors can be used to divide the fibre into sensor sections. The sensor might find application for damage detection, dynamic analysis, modal behaviour, load cycle and fatigue monitoring in the civil engineering field as well as industry, infrastructure, transportation and aeronautics. Its robustness against changes of the reflected optical power and the possibility to simultaneously measure optical power changes at the reflection points provide a great versatility of applications. We are confident that continued improvements of signal processing and measurement setup will further enhance the accuracy and measurement speed of the sensor system.

References

- [1] Thevenaz L 2006 Review and progress in distributed fiber sensing *Proc. Optical Fiber Sensors OSA Technical Digest (CD) ThC1* 1–6
- [2] Froggatt M and Moore J 1998 High-spatial-resolution distributed strain measurement in optical fiber with Rayleigh scatter *Appl. Opt.* **37** 1735–40
- [3] Posey R, Johnson G A and Vohra S T 2000 Strain sensing based on coherent Rayleigh scattering in an optical fibre *Electron. Lett.* **36** 1688–9
- [4] Liehr S, Lenke P, Wendt M, Krebber K, Seeger M, Thiele E, Metschies H, Gebreselassie B and Münich J C 2009 Polymer optical fiber sensor for distributed strain measurement and application in structural health monitoring *IEEE Sensors J.* **9** 1330–8
- [5] Liehr S, Nöther N and Krebber K 2010 Incoherent optical frequency domain reflectometry and distributed strain detection in polymer optical fibers *Meas. Sci. Technol.* **21** 017001
- [6] Liehr S, Wendt K and Krebber K 2009 Distributed perfluorinated POF strain sensor using OTDR and OFDR techniques *Proc. SPIE* **7503** 75036G-1–4
- [7] Inaudi D 2004 SOFO sensors for static and dynamic measurements *1st FIG Int. Symp. on Engineering Surveys for Construction Works and Structural Engineering*
- [8] Bachmann A, Lubert M, Poisel H and Ziemann O 2008 Strain sensor using phase measurement techniques in polymer optical fibers *Proc. SPIE* **7004** 70041N
- [9] Nöther N, Wosniok A, Krebber K and Thiele E 2009 A distributed fiber-optic sensor system for monitoring of large geotechnical structures *Proc. 4th Int. Conf. of Structural Health Monitoring of Intelligent Infrastructure SHMII-4*